Constrained finite-control-set predictive control of an H-bridge direct current motor drive

Bouiri Abdesselam[1], Kendzi Mohammed[2], Boughazi Othmane[3], Draoui Abdelghani[1]
[1]Faculty of Science and Technology, University of Tindouf, Tindouf, Algeria
[2]Institute of Science and Technology, University Center Salhi Ahmed Naama, Naama, Algeria
[3]Laboratory of Smart Grids and Renewable Energies, Department of Electrical Engineering, University of Bechar, Bechar, Algeria

Article Info

Article history:

Received Feb 28, 2026
Revised Jul 3, 2026
Accepted Aug 28, 2026

Keywords:

Cost function
Current constraint
DC motor drive
Finite control set
H-bridge converter

ABSTRACT

This paper presents a constrained finite-control-set model predictive control (FCS-MPC) scheme for an H-bridge converter-fed direct current (DC) motor drive, aimed at fast dynamic response and low steady-state armature-current ripple. By selecting the converter switching state directly at each sampling instant, the method removes the separate pulse-width modulation (PWM) stage used in conventional cascaded proportional-integral (PI) control and embeds the armature-current limit directly in the cost function. When the predicted armature current exceeds the predefined limit, a penalty term drives the optimizer to choose the sw itching state that returns the current within safe bounds while preserving speed tracking. The controller is evaluated in simulation under fixed-speed reference tracking, variable-speed reference tracking, and a step load-torque disturbance. The results show fast settling, low steady-state speed error, and bounded current during transients; under the idealized simulation conditions the steady-state armature-current total harmonic distortion (THD) is 0.21 %, indicating low current ripple for the studied operating points. The present study is limited to simulation; experimental validation and a quantitative comparison against conventional PI-PWM control are identified as future work.

Corresponding Author:

Bouiri Abdesselam
Faculty of Science and Technology, University of Tindouf, Algeria
Al-Mustaqbal District, P.O. Box 37000, Tindouf, Algeria
Email: abdesselam.bouiri@cuniv-tindouf.dz

1. INTRODUCTION

Direct current (DC) motor drives are widely used in the industrial and electromechanical field due to their simplicity, high starting torque and good control characteristics. Although alternating current (AC) machines are preferred in many modern applications, the DC motor is still preferred in smooth low speed operation and quick dynamic response applications. In power electronic systems, the DC motor is often used in H-bridge structures in order to provide bidirectional voltage control and four-quadrant operation [1], [2]. Power electronic systems combined with modern control methods provide improved performance, efficiency and flexibility for DC drive applications.

The conventional control approaches for DC motor drive are based on cascaded proportional–integral (PI) regulators and pulse-width modulation (PWM) techniques. Although PWM is easy to implement and provides fixed-frequency switching, it has a number of drawbacks. The cascaded control structure requires a large number of adjustable parameters [3], [4], to be set and, after a change in load or due to parameter drifts, the transient response is often very sluggish. Also, as the modulation and control actions are performed in a separate manner, the system constraints and nonlinear behavior cannot be directly taken into account in the controller design [5]. As drive systems evolve toward higher performance requirements, these limitations motivate the exploration of more advanced control strategies.

Model predictive control (MPC) has been increasingly applied in power electronics and electrical drives because of its conceptual simplicity and its explicit handling of constraints [6]–[9]. Finite-control-set MPC (FCS-MPC) has attracted particular interest because it operates directly on the discrete switching states of the power converter [6], [10]. Rather than computing modulator reference signals, the controller considers all admissible switching states and selects the optimal one by minimizing a cost function at each sampling instant. In this way the PWM stage is removed, and current, voltage, and switching constraints can be incorporated directly into the optimization [7], [11].

Among its advantages, FCS-MPC offers a fast-transient response, strong disturbance rejection, a control structure without an explicit modulator, and a flexible cost-function design [6], [10]. In many power-electronic and motor-drive applications, predictive control provides better dynamic performance than conventional PI-PWM control [11]–[13]. Because FCS-MPC accounts for the converter switching states explicitly, it is well suited to the H-bridge-fed DC motor, where the number of possible switching states is small and finite, so the optimization over all candidate states remains computationally light.

Most reported FCS-MPC studies target AC drives, grid-connected inverters, and multilevel converters, where reducing current harmonics and torque ripple is an active research area [14]–[16]. By contrast, the constrained FCS-MPC of an H-bridge-fed DC motor drive, in which the armature-current limit is enforced inside the cost function and the resulting steady-state current quality is analyzed across different load-torque conditions, has received comparatively little attention. This work addresses that gap. Its contribution is a single-objective FCS-MPC cost function that combines speed tracking with an explicit, switchable armature-current constraint for an H-bridge DC drive, together with a steady-state harmonic analysis of the resulting armature current under fixed-speed, variable-speed, and load-disturbance operation.

This paper presents a constrained FCS-MPC strategy for a DC motor fed by an H-bridge converter, as shown in Figure 1. First, a discrete-time prediction model for the armature current and speed is derived. A cost function that combines speed-tracking performance with armature-current limitation is then constructed, and a constraint-based switching-selection rule is designed to keep the current within safe bounds under load disturbance. Finally, the proposed method is verified through simulation under fixed-speed tracking, variable-speed tracking, load-torque variation, and steady-state harmonic analysis.

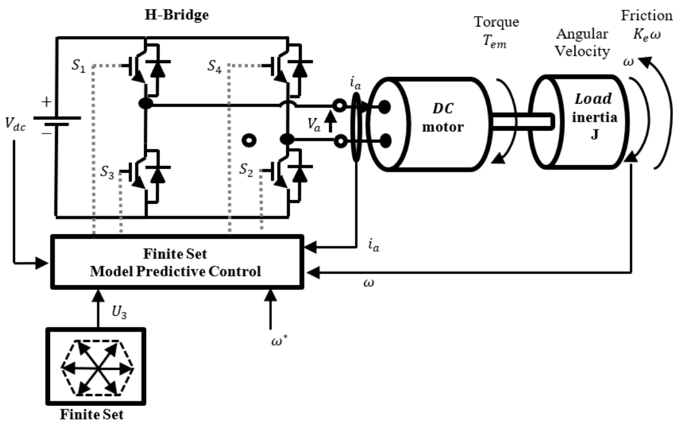

Figure 1. System configuration of a finite set MPC H-bridge fed DC motor drive

2. SYSTEM MODELING

The DC motor is modeled using classical electrical and mechanical dynamic equations derived from Kirchhoff's voltage law and Newton's second law [4]–[7], [10]–[12], [17].

2.1. Electrical and mechanical equation

Applying Kirchhoff's voltage law to the armature circuit gives:

$$v_a = R_a\, i_a + L_a \frac{di_a}{dt} + e_{mf} \tag{1}$$

$$e_{mf} = K_e \omega \tag{2}$$

$$J\frac{d\omega}{dt} + B\omega = T_{em} - T_L \quad (3)$$

$$T_{em} = K_t i_a \quad (4)$$

where:
a. v_a: motor armature voltage
b. i_a: armature current
c. e_{mf}: back electromotive force (back-EMF)
d. ω: rotor speed
e. T_{em}: electromagnetic torque developed by the motor
f. T_L: load torque
g. R_a , L_a: armature resistance and inductance
h. K_e, K_t: back-EMF and torque constants
i. J, B: inertia and viscous friction coefficients

The (1)-(4) represent the complete continuous-time dynamic model of the DC motor [17], [18].

2.2. H-bridge converter model

2.2.1. Switching states and output voltage

A full H-bridge converter consists of four controlled switches allowing bidirectional voltage application to the DC motor [1], [2]. The switching function $S \in \{+1, -1\}$ defines the applied voltage:

$$v_a = S.V_{dc} \quad (5)$$

where: $S = +1$ forward voltage, $S = -1$ reverse voltage, and V_{dc} is the DC supply voltage. Thus, the converter has a finite control set of two possible voltage vectors, which makes it suitable for FCS-MPC implementation [6], [10].

2.2.2. Discrete-time formulation

For predictive control, the continuous model must be discretized using sampling time T_s Using forward Euler approximation applying to (6), (7) [19]:

$$i_a(k+1) = i_a(k) + \frac{T_s}{L_a}[V_a(k) - R_a i_a(k) - K_e\omega(k)] \quad (6)$$

$$\omega(k+1) = \omega(k) + \frac{T_s}{J}[K_t i_a(k) - B\omega(k) - T_L(k)] \quad (7)$$

These discrete equations are used to predict future current and speed values for each possible switching state of the H-bridge [6], [10], [11]. The controller evaluates the predicted states for $S = +1$ and $S = -1$ and selects the switching state that minimizes the defined cost function.

3. PROPOSED FCS-MPC STRATEGY

The FCS-MPC in Figure 2 operates directly on the discrete switching states of the power converter. At each sampling instant, FCS-MPC evaluates the predicted system response for every admissible switching state and selects the state that minimizes a cost function [10], [11]. Because the optimal state is applied directly to the converter, the modulation stage of conventional PWM control is eliminated, and the switching decision is obtained by solving the optimization problem online within each sampling period [20], [21].

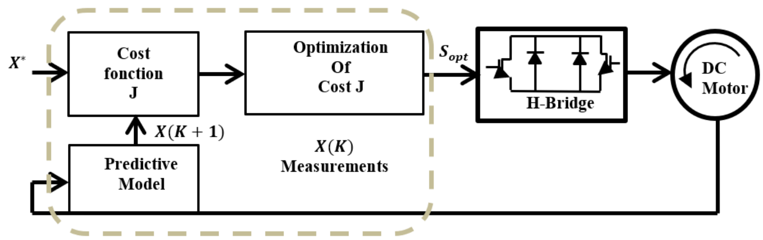

Figure 2. Block diagram of MPC for a DC motor drive

3.1. Prediction model

The predictive controller uses the discrete-time model derived in section 2.2.2. Using a sampling period Ts, the forward Euler discretization yields:

$$i_a(k+1) = i_a(k) + \frac{T_s}{L_a}[V_a(k) - R_a i_a(k) - K_e\omega(k)] \tag{8}$$

$$\omega(k+1) = \omega(k) + \frac{T_s}{J}[K_t i_a(k) - B\omega(k) - T_L(k)] \tag{9}$$

At each sampling instant k, the controller evaluates the two possible switching states of the H-bridge:

$$v_a(k) \in \{+Vdc, -Vdc\} \tag{10}$$

For each candidate switching state, predicted current $i_a(k+1)$ and speed $\omega(k+1)$ are computed using (8) and (9). This one-step-ahead prediction principle is the core of FCS-MPC applied to power converters and electrical drives [10], [11].

3.2. Cost function formulation

The optimal switching state is selected by minimizing a cost function J, designed to achieve speed tracking while limiting armature current.

a. Speed tracking term

The primary control objective is speed tracking:

$$J_\omega = \lambda_\omega(\omega^*(k+1) - \omega(k+1))^2 \tag{11}$$

where ω^* is the reference speed.

b. Current penalty term

To prevent excessive armature current, a current penalty term is introduced, following the constraint-handling principle used in current- and torque-limited predictive drives [22], [23]:

$$J_i = \lambda_i(i_a(k+1))^2 \tag{12}$$

where λ_i is a weighting factor that determines the trade-off between speed performance and current limitation.

c. Total cost function

The total cost function becomes:

$$J = J_\omega + J_i \tag{13}$$

$$J = \lambda_\omega(\omega^*(k+1) - \omega(k+1))^2 + \lambda_i(i_a(k+1))^2 \tag{14}$$

The weighting factors determine the relative priority of the two competing objectives. A larger λ_ω emphasizes speed-tracking accuracy and yields a faster transient response, but it allows larger armature-current excursions during transients; a larger λ_i penalizes current more strongly, limiting current stress and improving protection of the switches at the cost of a slower speed response. In this work λ_ω and λ_i were selected so that speed tracking dominates under normal operation while the current term remains active enough to bound transient current, with the hard limit enforced separately by the constraint term in (17). Because the two objectives are expressed in different physical units, the factors also perform normalization; their selection therefore directly affects both tracking performance and robustness to load variation, and is commonly tuned offline as discussed in [21]. The switching state minimizing (14) is applied during the next sampling interval.

d. Current constraint algorithm

Although the penalty term reduces current magnitude, strict safety constraints may require explicit current limitation. Activation mechanism, a current threshold I_{max} is defined:

$$| i_a(k+1) | > i_{max} \tag{15}$$

This ensures hard constraint satisfaction, consistent with constrained MPC theory [11], [24], [25].

e. Constraint-based current absorption strategy

When overcurrent is predicted, the controller selects the switching state that: minimizes speed error and forces current decay toward safe limits. In a DC motor fed by an H-bridge, selecting the opposite voltage polarity naturally produces current reduction due to the motor inductance:

$$\frac{di_a}{dt} \approx \frac{1}{L_a}(-R_a\, i_a + K_e\omega) \tag{16}$$

This strategy is based on controlling the currents to meet the voltage in the least time and without the need for additional peripherals, a feature that is in line with the constraints handled by predictive control. [10], [21]. When the constraint is activated, the cost function is modified as:

$$J = \begin{cases} J, & |\, i_a(k+1)\,| < i_{max} \\ J + \lambda_C(|\, i_a(k+1)\,| - i_{max})^2, & |\, i_a(k+1)\,| \geq i_{max} \end{cases} \tag{17}$$

where λ_c is a large penalty factor.

3.3. Optimization procedure

The optimal control action is selected as:

$$V_a{}^{opt}(k) = \underset{V_a(k)\in U_3}{\arg}\ \min J \tag{18}$$

This is the block diagram Figure 3 of the FCS-MPC for the H-bridge-fed DC motor, where the present current and speed values are given to the predictive model to predict the future current and speed values. Based on the predictive values, a cost function is computed and sent to the optimizer. In this case, the optimizer is focused on minimizing the cost function while considering the current constraints. After minimizing the cost function, the optimal switch signals are sent to the H-bridge in order to obtain the desired speed in the DC motor.

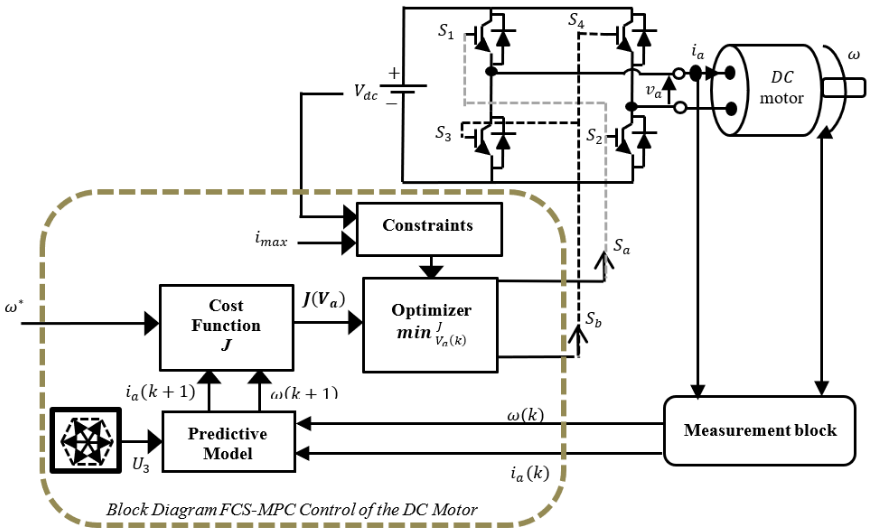

Figure 3. Block diagram of FCS-MPC for a DC motor drive

This real-time optimization is performed without a modulator: the controller handles the current constraint directly, provides a fast-transient response, and offers flexibility in shaping the cost function [10], [20], [21]. Regarding computational cost, the H-bridge admits only two admissible switching states ($S = +1$ and $S = -1$). At each sampling instant the controller therefore evaluates the prediction (8)-(9) and the cost function (14) twice and applies one comparison, so the per-step burden is small and constant. This finite, low-cardinality control set is a practical advantage over AC-drive FCS-MPC, where the number of candidate voltage vectors is considerably larger.

4. RESULTS AND DISCUSSION

The proposed FCS-MPC strategy for the H-bridge-fed DC motor drive is evaluated through dynamic and steady-state simulation. The DC motor and controller parameters used in all simulations are summarized in Table 1. The following subsections examine speed tracking, current regulation, and torque response under fixed-speed reference tracking, variable-speed reference tracking, and a step load-torque disturbance.

Table 1. Performance indices of the proposed FCS-MPC controller

Performance index	Proposed FCS-MPC	PI-PWM (baseline)
Speed root mean square error (RMSE) (rad/s)	0.1842	2.9465
Speed integral of squared error (ISE) (rad²·s)	0.0217	1.3842
Settling time (s)	0.1980	0.4620
Peak start-up current (A)	48.60	71.35
Steady-state current total harmonic distortion (THD) (%)	0.21	3.84

4.1. Test: fixed-speed reference tracking

Figure 4 shows the speed-tracking performance of the FCS-MPC controller under a constant set-point speed of 100 rad/s. As shown in Figure 4(a), the motor speed rises smoothly from rest to the set-point within a short time (approximately 0.2 s) without overshoot and with low steady-state tracking error. This indicates that minimizing the predefined cost function yields accurate speed tracking, as also reflected by the small speed error in Figure 4(b).

Figure 4(c) shows the armature-current dynamics during start-up and regulation for the 0–100 rad/s transition. The initial peak corresponds to the acceleration torque required at start-up; the current constraint in the predictive model then becomes active and limits the current to the predefined value. In steady state, the current is nearly ripple-free and tracks its reference. Similarly, as shown in Figure 4(d), the torque exhibits a transient peak and then settles without sustained oscillation. Finally, the armature voltage in Figure 4(e) shows the expected discrete waveform produced by the FCS structure of the FCS-MPC. Overall, the speed response is fast and the steady-state speed error is low.

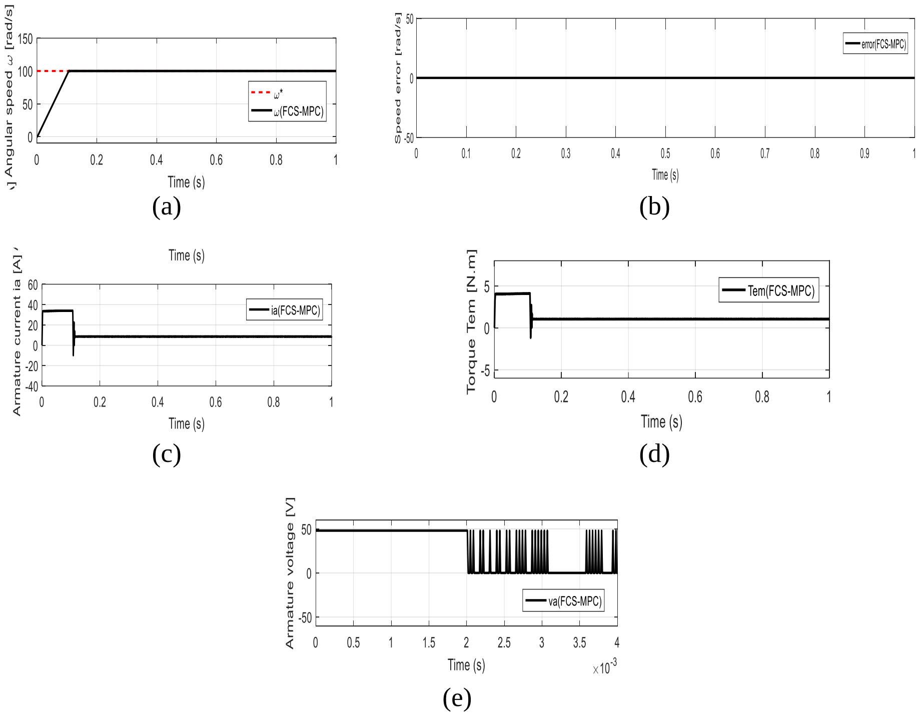

Figure 4. Dynamic performance of the DC motor drive under fixed-speed reference tracking using the proposed FCS-MPC controller: (a) motor angular speed and reference, (b) speed tracking error, (c) armature current and reference, (d) electromagnetic torque, and (e) armature-voltage switching

4.2. Test: variable reference tracking

In Figure 5, the reference speed is changed in a step-by-step manner to assess the dynamic tracking ability of the FCS-MPC controller. As observed in Figure 5(a), the actual speed tracks very quickly and accurately to the new desired reference speed in each step change, with zero steady-state error. The ability of the controller to track the reference speed accurately in both ascending and descending trajectories with no overshoot or oscillations confirms its robustness to changing references.

As shown in Figure 5(b) and Figure 5(c), the armature current and electromagnetic torque rise immediately after each step-in order to supply the required torque. These peaks are bounded by the current constraint enforced within the predictive controller. After a short transient, they settle at the steady-state values corresponding to the new operating point. The armature voltage in Figure 5(d) switches between the two discrete levels, as expected from the FCS-MPC approach. The fast settling, bounded current, and low steady-state speed error under reference changes indicate that the controller tracks both ascending and descending references without significant overshoot. Finally, Figure 5(e) shows the speed tracking error, which remains close to zero during steady-state operation, with only short-duration deviations during the reference transitions. The small and rapidly decaying tracking error further confirms the accurate and robust tracking capability of the proposed FCS-MPC controller under variable reference conditions.

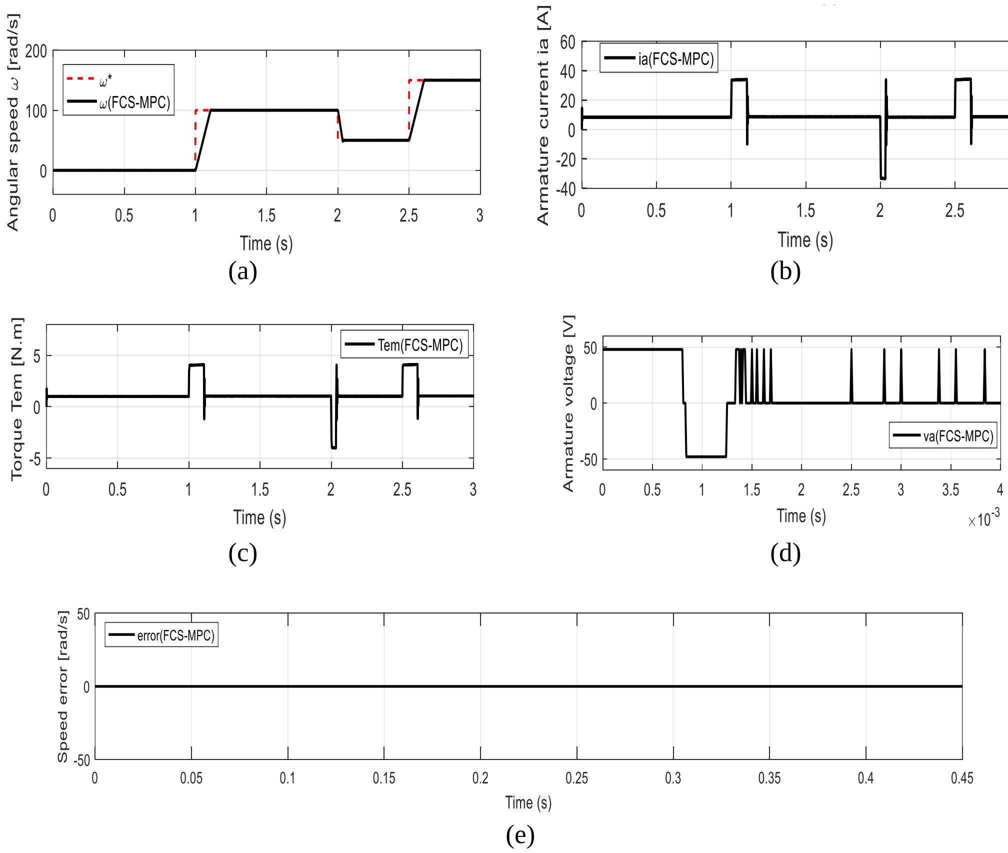

Figure 5. Dynamic performance of the DC motor drive under variable reference tracking using the proposed FCS-MPC controller: (a) angular speed, (b) armature current, (c) electromagnetic torque, (d) armature voltage, and (e) speed tracking error

4.3. Test: load disturbance rejection

In this scenario (Figure 6), a step change in load torque from 1 N·m to 10 N·m is applied at t = 0.2 s to verify the disturbance-rejection capability of the FCS-MPC controller. As shown in Figure 6(a), the angular speed deviates slightly at the instant of the change and then recovers quickly to the reference value. The zoomed speed response in Figure 6(b) shows a small peak deviation and a low steady-state error, indicating good robustness to sudden load changes.

The armature current and torque increase during the transient after the load step to supply the additional torque demand, as shown in Figure 6(c) and Figure 6(d). The transient current and torque peaks are bounded by the current constraint in the predictive controller. Figure 6(e) shows that the speed tracking error remains close to zero, with only a small transient deviation during the load change, further confirming the effective disturbance rejection of the proposed controller. Owing to the FCS approach, the armature voltage in Figure 6(f) continues to switch between the permissible voltage levels. In summary, the FCS-MPC scheme provides a fast response to the load disturbance while keeping the torque tracking stable. To complement the qualitative discussion above, the controller performance is summarized quantitatively in Table 2 using standard indices: the ISE and RMSE of the speed, the settling time, the peak armature current during the start-up transient, and the steady-state armature-current THD.

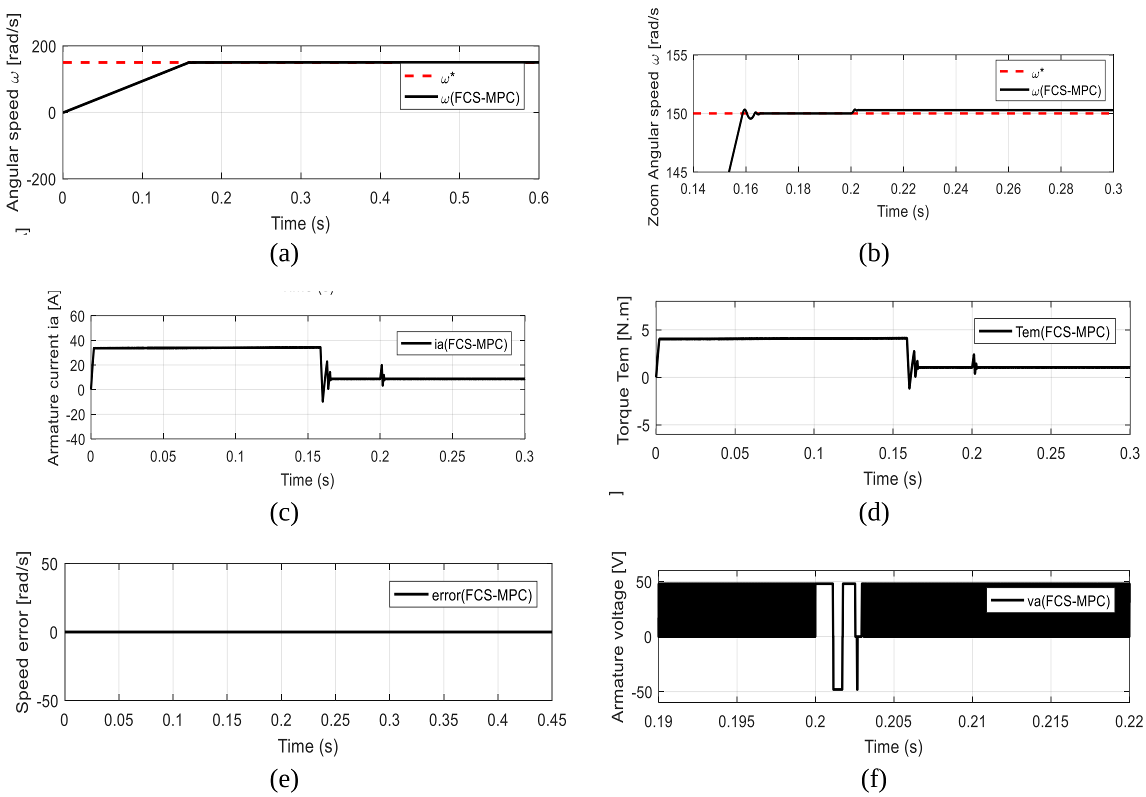

Figure 6. Dynamic performance of the DC motor drive under step load disturbance (1 N·m to 10 N·m at 0.2 s) using the proposed FCS-MPC controller: (a) angular speed, (b) zoomed angular speed, (c) armature current, (d) electromagnetic torque, (e) speed tracking error, and (f) armature voltage

Table 2. DC motor and system parameters

Parameter	Symbol	Value
Armature resistance	Ra	0.35 Ω
Armature inductance	La	2.5 mH
Torque constant	Kt	0.12 N·m/A
Back-EMF constant	Ke	0.12 V·s/rad
Rotor inertia	J	0.0032 kg·m²
Viscous friction coefficient	B	0.00032 N·m·s/rad
Rated speed	Ω	3000 rpm
DC bus voltage	Vdc	48 V
Load torque range	TL	1–3 N·m
Sampling time	Ts	100 µs

4.4. Steady-state current ripple and harmonic analysis

The steady-state armature-current ripple is examined to assess the current quality of the proposed scheme. Figure 7 shows the armature-current waveform after the transients have decayed; the ripple about the mean value is small. Under the idealized simulation conditions of this study, the computed THD of the steady-state armature current is 0.21 %. This value should be interpreted in context: it is obtained from a simulation in which the converter switches are ideal, the DC-link voltage is constant, and the large armature inductance strongly filters the current ripple. Because the FCS-MPC switching frequency is not fixed but depends on the sampling time and operating point, the absolute THD is sensitive to the sampling time used; a higher value is expected in a hardware implementation that includes dead time, measurement noise, and finite switching transitions.

The FFT spectrum of the steady-state ripple is shown in Figure 7. The spectral content is concentrated around the effective switching frequency and its multiples, while the low-frequency harmonics are small. This distribution is consistent with the behavior of FCS-MPC, whose variable switching frequency spreads the switching energy over a band rather than concentrating it at a single fixed harmonic. The low magnitude of the low-order harmonics indicates that the predictive scheme maintains good steady-state current quality for the studied operating points.

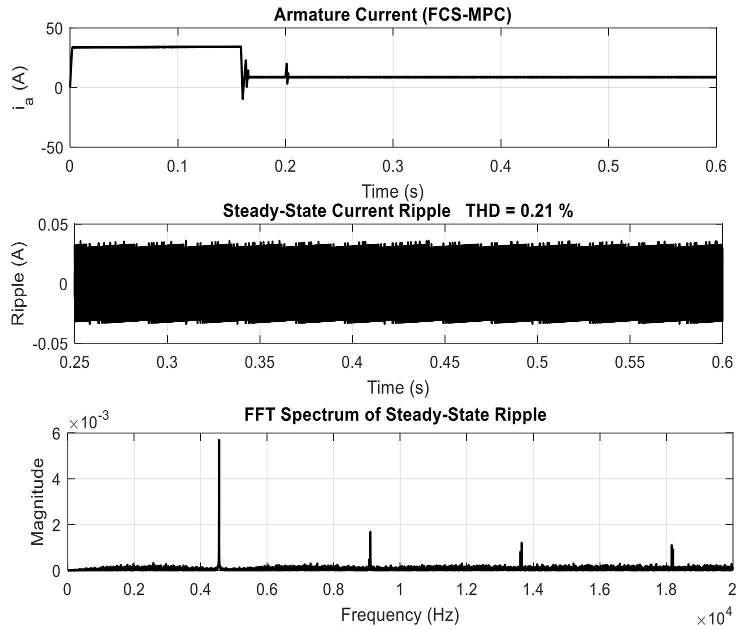

Figure 7. Armature current waveform, steady-state ripple, and FFT spectrum showing THD performance under FCS-MPC control

5. CONCLUSION

This paper proposed a constrained FCS-MPC strategy for an H-bridge converter-fed DC motor drive. The method uses a discrete-time prediction model of the armature current and rotor speed, derived from the electrical and mechanical equations of the motor, and a cost function that combines speed tracking with an explicit, switchable armature-current constraint. The main contributions are: (i) a single-step FCS-MPC formulation for the H-bridge DC drive that removes the PWM stage; (ii) an in-cost-function current-limiting mechanism that bounds the transient armature current without additional hardware; and (iii) a steady-state harmonic analysis of the armature current under fixed-speed, variable-speed, and load-disturbance operation. The simulation results show fast settling, low steady-state speed error, bounded transient current, and low steady-state current ripple under the studied conditions.

The present study has limitations. The results are obtained entirely in simulation under idealized conditions, and the reported current THD should be read in that context. A direct quantitative comparison against a conventional PI-PWM controller, and against other predictive schemes, was not yet carried out. Future work will therefore focus on: (i) a quantitative benchmarking of the proposed scheme against PI-PWM and alternative MPC strategies, (ii) experimental validation on a laboratory H-bridge DC-drive prototype including switching non-idealities and measurement noise, and (iii) extension to multi-step prediction and to robustness analysis under parameter mismatch.

FUNDING INFORMATION

Authors state no funding involved.

AUTHOR CONTRIBUTIONS STATEMENT

This journal uses the Contributor Roles Taxonomy (CRediT) to recognize individual author contributions, reduce authorship disputes, and facilitate collaboration.

Name of Author	C	M	So	Va	Fo	I	R	D	O	E	Vi	Su	P	Fu
Bouiri Abdesselam	✓	✓	✓	✓	✓	✓		✓	✓	✓			✓	
Kendzi Mohammed		✓		✓	✓	✓		✓		✓	✓			
Boughazi Othmane	✓		✓	✓			✓			✓	✓	✓		✓
Draoui Abdelghani		✓		✓	✓		✓			✓		✓	✓	

C : **C**onceptualization
M : **M**ethodology
So : **So**ftware
Va : **Va**lidation
Fo : **Fo**rmal analysis
I : **I**nvestigation
R : **R**esources
D : **D**ata Curation
O : Writing - **O**riginal Draft
E : Writing - Review & **E**diting
Vi : **Vi**sualization
Su : **Su**pervision
P : **P**roject administration
Fu : **Fu**nding acquisition

CONFLICT OF INTEREST STATEMENT

Authors state no conflict of interest.

DATA AVAILABILITY

The data supporting the findings of this study are available within the article. Additional simulation data and model parameters are available from the corresponding author upon reasonable request.

REFERENCES

[1] R. W. Erickson and D. Maksimović, *Fundamentals of Power Electronics*. Boston, MA: Springer US, 2001. doi: 10.1007/b100747.

[2] N. Mohan, T. M. Undeland, and W. P. Robbins, *Power Electronics: Converters, Applications, and Design*, 3rd ed. Hoboken, NJ, USA: Wiley, 2003.

[3] J. Holtz, "Pulsewidth Modulation for Electronic Power Conversion," *Proceedings of the IEEE*, vol. 82, no. 8, pp. 1194–1214, 1994, doi: 10.1109/5.301684.

[4] K. Ogata, *Modern Control Engineering*, 5th ed. Upper Saddle River: Pearson, 2010.

[5] S. J. Qin and T. A. Badgwell, "A survey of industrial model predictive control technology," *Control Engineering Practice*, vol. 11, no. 7, pp. 733–764, Jul. 2003, doi: 10.1016/S0967-0661(02)00186-7.

[6] S. Kouro, P. Cortés, R. Vargas, U. Ammann, and J. Rodríguez, "Model predictive control - A simple and powerful Method to control power converters," *IEEE Transactions on Industrial Electronics*, vol. 56, no. 6, pp. 1826–1838, Jun. 2009, doi: 10.1109/TIE.2008.2008349.

[7] S. Vazquez, J. Rodriguez, M. Rivera, L. G. Franquelo, and M. Norambuena, "Model Predictive Control for Power Converters and Drives: Advances and Trends," *IEEE Transactions on Industrial Electronics*, vol. 64, no. 2, pp. 935–947, 2017, doi: 10.1109/TIE.2016.2625238.

[8] C. Li, Q. Meng, and T. Shi, "A review on model predictive control strategies for AC motor drives," *IET Electric Power Applications*, vol. 18, no. 11, pp. 1584–1604, Nov. 2024, doi: 10.1049/elp2.12510.

[9] M. B. Shahid *et al.*, "Model predictive control for energy efficient AC motor drives: An overview," *IET Electric Power Applications*, vol. 18, no. 12, pp. 1894–1920, Dec. 2024, doi: 10.1049/elp2.12517.

[10] J. Rodriguez and P. Cortes, "Predictive Control of Power Converters and Electrical Drives." *Wiley*, Mar. 15, 2012. doi: 10.1002/9781119941446.

[11] P. Cortés, M. P. Kazmierkowski, R. M. Kennel, D. E. Quevedo, and J. Rodriguez, "Predictive control in power electronics and drives," *IEEE Transactions on Industrial Electronics*, vol. 55, no. 12, pp. 4312–4324, Dec. 2008, doi: 10.1109/TIE.2008.2007480.

[12] D. Q. Mayne, J. B. Rawlings, C. V. Rao, and P. O. M. Scokaert, "Constrained model predictive control: Stability and optimality," *Automatica*, vol. 36, no. 6, pp. 789–814, Jun. 2000, doi: 10.1016/S0005-1098(99)00214-9.

[13] T. Li, X. Sun, G. Lei, Y. Guo, Z. Yang, and J. Zhu, "Finite-Control-Set Model Predictive Control of Permanent Magnet Synchronous Motor Drive Systems - An Overview," *IEEE/CAA Journal of Automatica Sinica*, vol. 9, no. 12, pp. 2087–2105, Dec. 2022, doi: 10.1109/JAS.2022.105851.

[14] A. A. Abdel-Aziz, M. A. Elgenedy, and B. W. Williams, "Model Predictive Current Control for Low-Cost Shunt Active Power Filter," *CSEE Journal of Power and Energy Systems*, vol. 10, no. 4, pp. 1589–1598, 2024, doi: 10.17775/CSEEJPES.2023.00570.

[15] Z. Xue, S. Niu, A. M. H. Chau, Y. Luo, H. Lin, and X. Li, "Recent Advances in Multi-Phase Electric Drives Model Predictive Control in Renewable Energy Application: A State-of-the-Art Review," *World Electric Vehicle Journal*, vol. 14, no. 2, p. 44, Feb. 2023, doi: 10.3390/wevj14020044.

[16] Q. Yang *et al.*, "A Fixed Switching Frequency Direct Model Predictive Control for Neutral-Point-Clamped Three-Level Inverters with Induction Machines," *IEEE Transactions on Power Electronics*, vol. 38, no. 11, pp. 13703–13716, Nov. 2023, doi: 10.1109/TPEL.2023.3300098.

[17] R. Krishnan, "Electric motor drives: Modeling, analysis and control," *International Journal of Robust and Nonlinear Control*, vol. 14, no. 8, pp. 767–769, 2004, doi: 10.1109/9780470545557.

[18] W. Leonhard, *Control of Electrical Drives*, 3rd ed. Berlin, Germany: Springer, 2001.

[19] K. J. Åström and B. Wittenmark, *Computer-controlled systems: theory and design*, 3rd ed. Mineola, NY, USA: Dover

Publications, 2011.

[20] T. Geyer, "A comparison of control and modulation schemes for medium-voltage drives: Emerging predictive control concepts versus PWM-based schemes," *IEEE Transactions on Industry Applications*, vol. 47, no. 3, pp. 1380–1389, May 2011, doi: 10.1109/TIA.2011.2127433.

[21] P. Karamanakos and T. Geyer, "Guidelines for the Design of Finite Control Set Model Predictive Controllers," *IEEE Transactions on Power Electronics*, vol. 35, no. 7, pp. 7434–7450, Jul. 2020, doi: 10.1109/TPEL.2019.2954357.

[22] I. D. De Martin, A. Brosch, F. Tinazzi, and M. Zigliotto, "Continuous Control Set Model Predictive Torque Control With Minimum Current Magnitude Criterion for Synchronous Motor Drives," *IEEE Transactions on Industrial Electronics*, vol. 71, no. 7, pp. 6787–6796, 2024, doi: 10.1109/TIE.2023.3308132.

[23] A. Brosch, O. Wallscheid, and J. Bocker, "Time-Optimal Model Predictive Control of Permanent Magnet Synchronous Motors Considering Current and Torque Constraints," *IEEE Transactions on Power Electronics*, vol. 38, no. 7, pp. 7945–7957, 2023, doi: 10.1109/TPEL.2023.3265705.

[24] J. B. Rawlings and D. Q. Mayne, "Model Predictive Control: Theory and Design," *Control*, vol. 57, no. 5, pp. 1040–50, 2010, [Online]. Available: http://www.pubmedcentral.nih.gov/articlerender.fcgi?artid=2935661&tool=pmcentrez&rendertype=abstract

[25] E. F. Camacho and C. Bordons, *Model Predictive control*. Springer London, 2nd ed. London, 2007. doi: 10.1007/978-0-85729-398-5.

BIOGRAPHIES OF AUTHORS

Bouiri Abdesselam is a Lecturer Professor at the University of Tindouf, Algeria. He received the B.Eng. and M.Eng. degrees in Electrical Engineering and Electric Networks from Tahri Mohammed University of Bechar, Algeria, in 2016 and 2018, respectively. He received the Ph.D. degree in Advanced Power Electronics from the same university in 2022. His main research interests include electrical machines, nonlinear control, power electronics, optimization algorithms, intelligent control, and renewable (wind and solar) energy. He can be contacted at email: abdesselam.bouiri@cuniv-tindouf.dz.

Kendzi Mohammed is an Assistant Professor at the University of Naama, Algeria. He received his B.S. degree in 2003 and his M.S. degree in 2012. He received his Ph.D. degree in Electrical Engineering from Tahri Mohammed University of Béchar, in 2020. His current research interests are: power electronics, control of electrical machines, artificial intelligence applications in control systems, renewable energy systems. He can be contacted at email: kendzimohammed@gmail.com.

Boughazi Othmane working since 2018 as a Lecturer Professor in the Department of Electrical Engineering at Tahri Mohammed University of Bechar, Algeria. The year 2006 brought his B.Eng. in Electrical Engineering from that same institution. By 2010, he had completed an M.Sc. He obtained his Ph.D. degree in Electrical Engineering from the same university in 2016. He is a member of the Smart Grid and Renewable Energy Laboratory (SGRE). His main research interests include electric machines and drive systems, power electronics, and process control. He can be contacted at email: boughazi.othmane@univ-bechar.dz.

Draoui Abdelghani is a Lecturer Professor at the University of Tindouf, Algeria. He received the B.Eng. and M.S. degrees in Electrical Engineering from the Institute of Electrical and Electronic Engineering (ex-INELEC), University of Boumerdes, in 2013 and 2015, respectively. He received his Ph.D. degree in Electric Power Engineering from the University of Bechar, Algeria, in 2019. His research interests include optimization, metaheuristics, renewable energy, power electronics, power generation, power grids, battery chargers, and artificial intelligence applied to power systems. He can be contacted at email: abdelghani.draoui@cuniv-tindouf.dz.